Chapter 16
Fluid and Thermal Analysis of Power Li-Ion Battery Pack and Experimental Verification

Dafen Chen, Jiuchun Jiang, Yaojuan Duan, Zhanguo Wang and Feng Wen

Abstract Fluid flow and heat transfer of a power li-ion battery pack which adopts the air cooling method with an electric fan are predicted using a computational fluid dynamics (CFD) software. The airflow rate distributions at coolant passages are analyzed quantificationally, which will affect temperature distribution of the battery pack. Temperatures at the center of battery surface that are located in the middle of each battery modules are monitored using thermal couples under the same driving cycle as simulation. The simulation results are close to the experimental ones, which indicate that the calculated results can be used as the basis of developing thermal management strategy of battery pack and optimization scheme of fluid flow.

Keywords Power li-ion battery pack · Thermal analysis · Fluid flow analysis

16.1 Introduction

Hybrid power traction locomotive (HPTL) can effectively reduce the fuel consumption and the associated emissions, which meets the national environment protection and energy policies. Therefore it has wide market prospects [1]. The component for energy storage in an HPTL mainly includes super capacitors, battery packs, and their combinations [2]. The energy storage component should have features of high specific energy and specific power, excellent high current

D. Chen (✉) · J. Jiang · Y. Duan · Z. Wang
National Active Distribution Network Technology Research Center (NANTEC), Beijing
Jiaotong University, Beijing, China
e-mail: 11117360@bjtu.edu.cn

F. Wen
Beijing Epower Electronic Co., LTD, Beijing, China

charge–discharge characteristics, long cycle life, environment friendly, and so on [3]. Because of its excellent performance, li-ion batteries become one of the most promising candidates of energy storage component in HPTLs. Actually, HPTLs such as HD300-910 already adopted li-ion battery packs as its energy storage device [4]. Generally, to ensure safety and cycle life of li-ion batteries, the environment temperature should be within the range of −25 to 55 °C during discharging and within 0–55 °C during charging [5]. Thus the cooling, heating, and thermal isolation schemes should be taken into account during designing of battery packs. Some researchers simulated the fluid and/or thermal fields of li-ion battery packs [6–9], but they barely verified the results in a real battery pack. In this paper, fluid and thermal fields of a power li-ion battery pack were simulated and we also monitored temperatures of a real battery pack to validate the simulation results.

16.2 Li-Ion Battery Pack Structure and CFD Model

The structure of the analyzed li-ion battery pack is shown in Fig. 16.1.

There are 88 batteries in the battery pack, which is connected in the way of 2 parallel and 44 series. They are divided into four modules, each module having 22 batteries. The modules are named as module A, module B, module C, and module D from inlet toward outlet. The gap between two batteries and the gap between battery and wall are all 1 mm. Each gap is an air passage, so there are 23 air passages in one module.

Because the battery pack structure is almost symmetry, in order to reduce calculation cost and running time, only half of the battery pack is constructed in the CFD model as in Fig. 16.2. Some geometrical features that are negligible for the fluid and thermal distribution are also simplified. When the fan is open, air from inlet flows to the bottom of battery modules, then flows through the air passages to the top of battery modules, and finally pumps out by the fan at the outlet. Between the bottom of battery modules, there are baffles with holes on them to change the airflow direction that makes the fluid distribution more uniform.

16.3 Flow Field Simulation Results of Battery Pack

Figures 16.3a,b show the airflow in the battery pack after the fan is started.

Because the area of inlet is relative smaller, the air velocity near inlet is higher than in other locations. The air from inlet is divided into four parts after it meets the baffles between module A and module B. The main part is squeezed to the ends of the baffles and flows into the next module. Another part flows through the gap in the batteries which is located in middle of module A and comes to the top of the battery pack directly; the third part forms a vortex, returning to the two corners
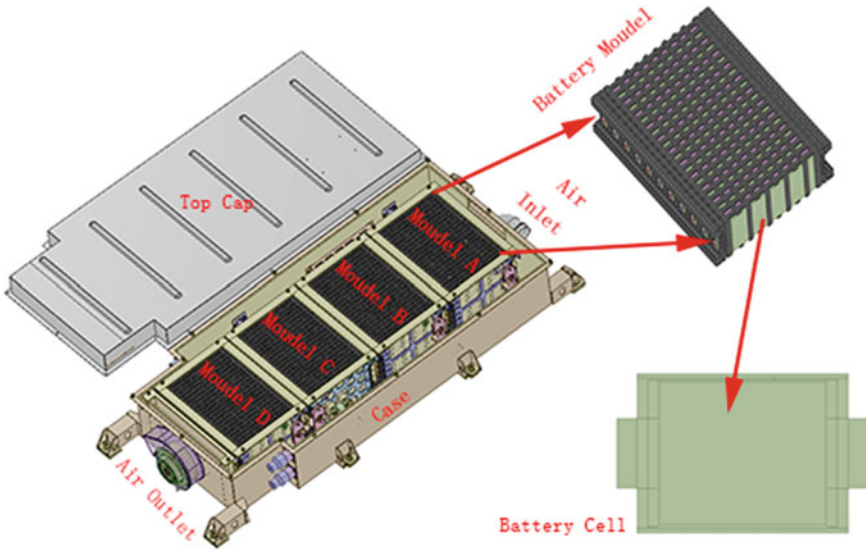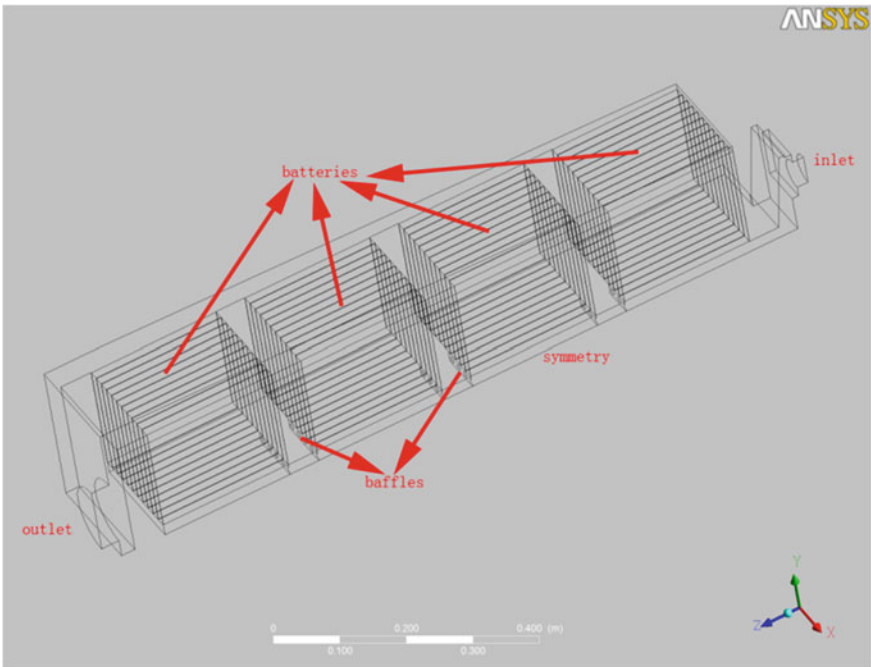
Fig. 16.1 Battery pack structure

Fig. 16.2 Simplified CFD model
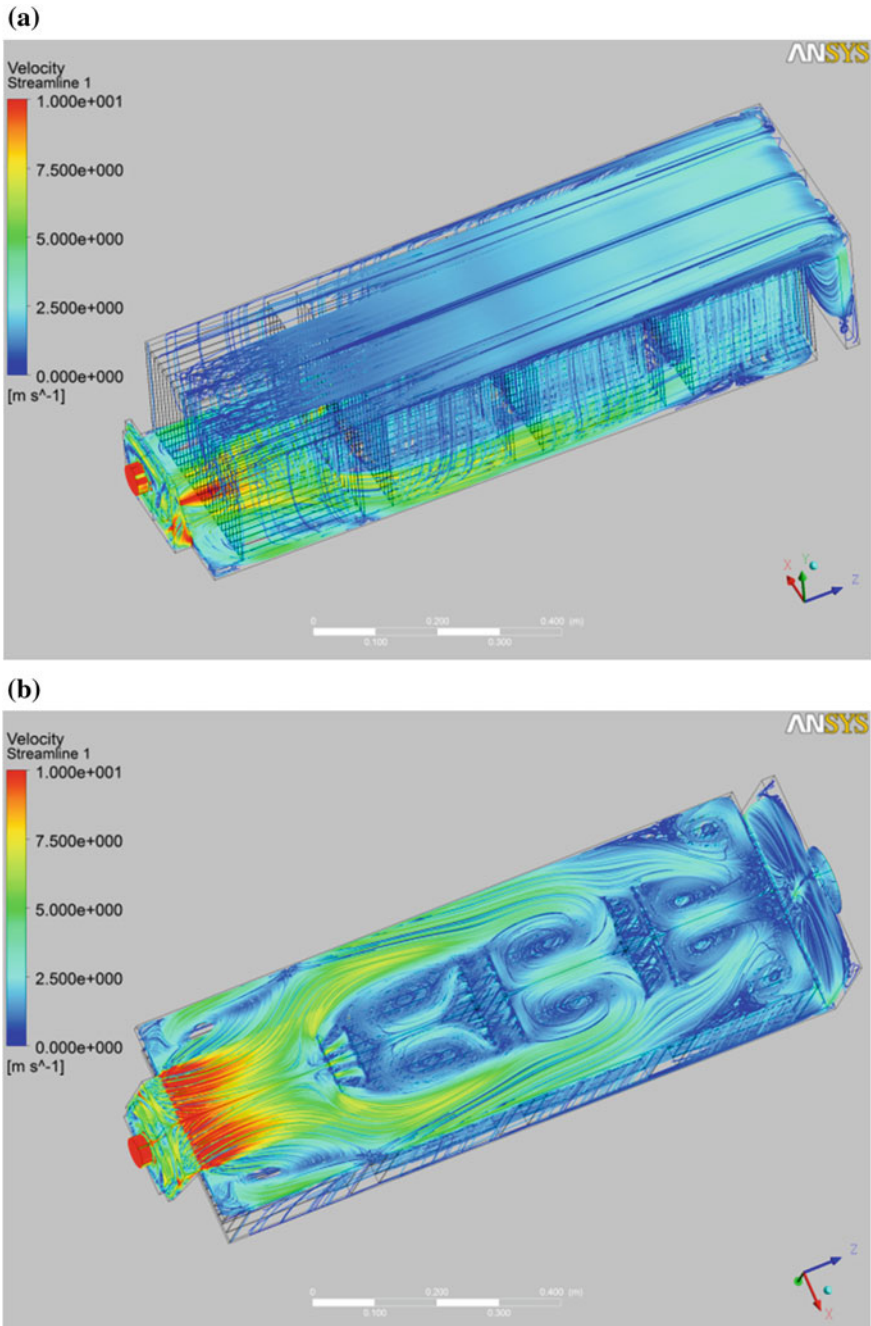
(a)

(b)

Fig. 16.3 **a** Streamline distribution in battery pack (*top view*). **b** Streamline distribution in battery pack (*bottom view*)

that are close to the inlet side and then flows to the top of module A; the rest flows through the holes on baffles into the module B directly.

Due to the block of baffles between modules A and B, the air that flows to other modules from the ends of the baffle has a relatively large velocity component that is perpendicular to the battery pack side walls. This velocity component leads airflow toward side walls. After rebounding by the wall, this part fluid has a velocity component in the direction pointing to symmetry plane. However, since part of the energy has been consumed during rebound, the velocity component is weakened. So the baffles between modules B and C capture a portion of the fluid flow back to the middle bottom of module B, and the baffles between modules C and D capture a portion of the fluid flow back to the middle bottom of module C, the part not captured by baffles flow to the bottom of module D.

The air at the top of modules is pumped out by the fan through a gradually increased air duct.

In order to regulate the battery temperature within a desired range and to reduce the battery cell to cell temperature variation in a battery pack, we often analyze the total flow rates and the uniformity of the fluid distribution. The fan parameters already fixed in this case can limit the temperature in the desired range sufficiently, so we mainly analyze the uniformity of the fluid field.

The heat dissipation power taken away by air that flows through the batteries gaps can be calculated as follows:

$$P_h = C_{air} q_{air} \left(\int_{A_{out}} T_{out} - \int_{A_{in}} T_{in} \right)$$

where P_h represents the heat dissipation power (J), C_{air} represents specific heat capacity of air (J/kg/ °C), q_{air} represents airflow rate(kg/s), T_{out} and T_{in} represent the air temperature at outlet and inlet surfaces respectively (°C).

Because all batteries are parallel from the view of airflow path in this battery pack, the capacity of heat dissipation is decided by the airflow rate. The airflow rates of all coolant passages are shown in Fig. 16.4.

The airflow rates are almost the same in modules C and D, while in modules A and B the airflow rates have a remarkable difference. The airflow rate is higher at the location near the side walls than the gaps located in the middle of module B. In module A, the gaps in the middle and two sides have higher airflow rates, while No.6 and No.19 air gaps have the lowest airflow rates. Module D has the highest total airflow rates, and module B has the lowest total airflow rates; the total airflow rates of module A are higher than module B and lower than module C. The unconformity of airflow rates at each coolant passages may lead to increase in the maximum temperature difference in battery pack, which will be analyzed in Sect. 16.4.
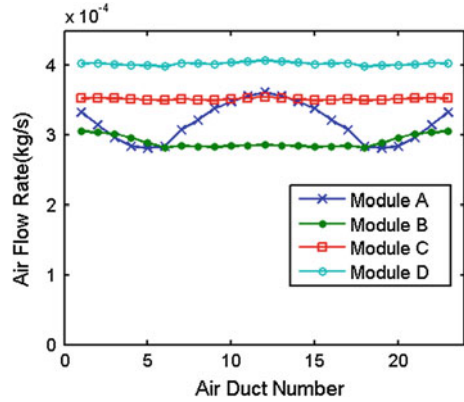
16.4 Thermal Field Simulation Results of Battery Pack

In order to verify whether the battery system can operate safely for a long time, the charge–discharge driving cycle at about SOC = 60 % (1C charge for 45 s and 1.5C discharge for 30 s) is simulated. The heat generation rate of single battery is calculated as follows:

$$P_{avg} = \frac{I_{chg}^2 R_{chg} t_{chg} + I_{dch}^2 R_{dch} t_{dch}}{t_{chg} + t_{dch}}$$

where P_{avg} is the average heat generate rate, I is the current, R is the total resistance, t is time, the subscript chg represents charge, and dch is discharge.

The initial temperature of battery pack is 27 °C and the fan is shut down. When the maximum temperature of the battery exceeds 40 °C the fan is started up. (approximately after the time is 6,000 s in the Simulation). The battery temperature distribution at the moment of the fan startup is shown in Fig. 16.5.

It can be seen from the figures that before the fan is on, the temperature difference is small; the highest temperature region is located at the top of modules A, B, and C; the cooler areas are the top of module D and the bottom of all modules. Because the top of module D is near the outlet side, its top space is the largest and the outlet air distance is shorter and the cooling capacity is stronger than other modules. Though the fan is off at this point, the bottom of the module temperature is lower because there is a certain airflow in the battery box and the hot airflow toward the tip. Because module A is near the air inlet and has heat exchange with the inlet air, thus the bottom of the battery module A has lower temperature than the bottom of other modules.

After the fan is started (Fig. 16.6a), the temperature of most regions in the battery system decreases due to forced air cooling; Because the airflow rate between the batteries is not equal, the temperature difference in the battery system increases; the hotter region corresponds to the small airflow rate area as shown in
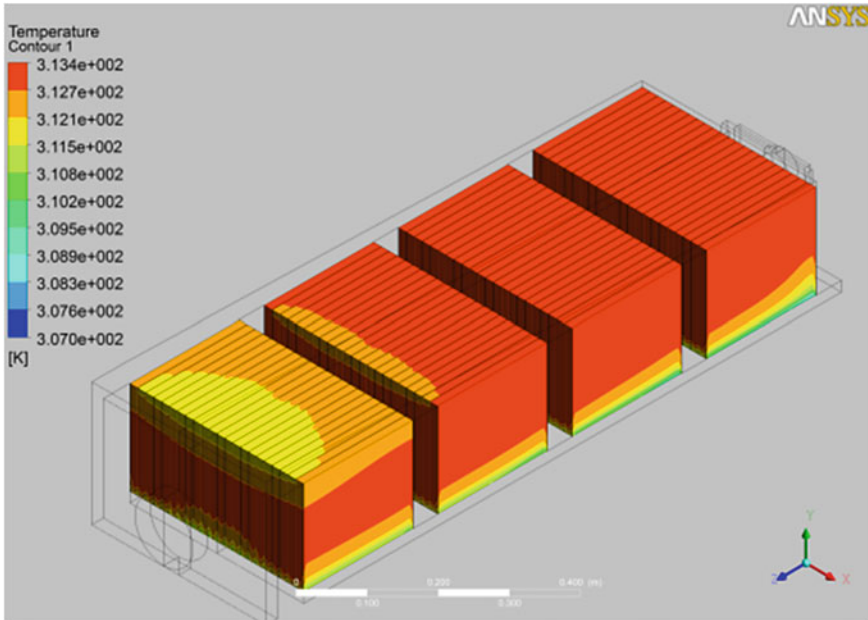
Fig. 16.5 The temperature distribution of battery surfaces at the moment of fan startup ($t = 6000$ s)

Fig. 16.4. The temperature at the bottom of the battery is lower, at the top temperature is higher, and the maximum temperature difference is about 8 °C (Fig. 16.6b).

Figure 16.7 shows the temperature curves of the center location at the surface of the battery which is located at the middle of each module. Before opening the fan, the temperature in different regions inside the battery pack is basically the same, while after turning on the fan, the significant temperature difference among the areas appears and the airflow rate is higher where the temperature is lower. The final temperature gap is about 3 °C.

16.5 Experimental Results and Discussion

Several temperature sensors are installed at the center of the each module in the actual battery pack, and the battery pack is charged and discharged using the same driving cycle condition with the set of the simulation conditions. Finally the temperature curve is obtained and shown as in Fig. 16.8a.

When the fan is shut down, the temperature difference of the battery at different modules is already obvious which may be due to the heat generated rates difference. After turning on the fan, the decline rate of temperatures shows that the
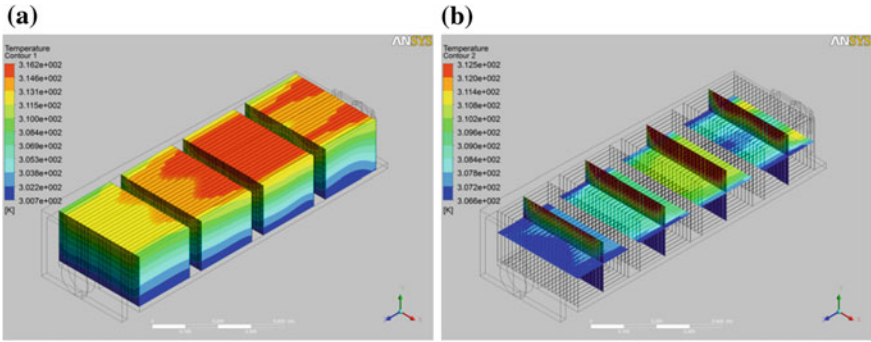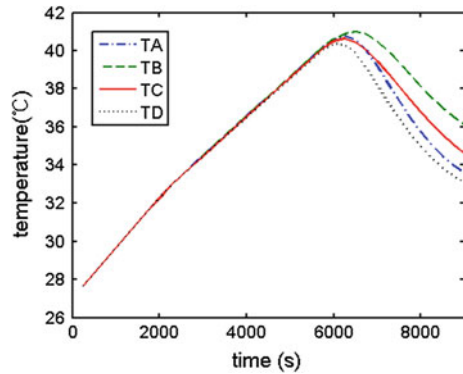
Fig. 16.6 a (*left*) The temperature distribution at battery surfaces after the fan startup 3,000 s (*t* = 9,000 s). **b** (*right*) The temperature difference inside batteries after the fan startup 3,000 s (*t* = 9000 s)

Fig. 16.7 Temperatures of each module center (simulate results)


temperature decline speed of module D is the fastest, temperature decline speed of module A and module C are almost the same, and module B is the worst.

As shown in Fig. 16.8b, the absolute error between simulation results and the experimental results is less than 4 °C, presenting that although the simulation ignores some factors including the part geometry of actual system, inconsistency between the batteries and the battery pack sealing, the simulated results are basically consistent with the experimental results.

16.6 Conclusion

A model of CFD is built to analyze the fluid field and thermal field of a power li-ion battery pack. The simulated results agreed well with the experimental results. From the simulation results we can conclude that: in battery pack that

Fig. 16.8 a Temperatures
of each module center
(experimental results).
b Temperature errors of
simulated and experimental
results
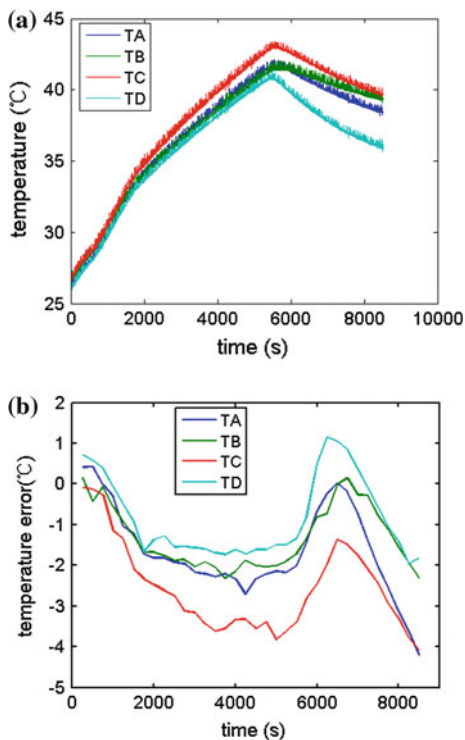
adopts parallel cooling construction, the fluid flow rate flow through each coolant
passage affects the thermal distribution directly, thus improved uniformity of the
fluid flow rate is very important. In addition, the inconsistency of batteries and the
seal condition will affect the distribution of fluid field and thermal field and should
be taken into account during battery pack design and manufacture.

References

1. Tian R, Kang Y (2012) Overview of the development of the hybrid locomotive at home and
   abroad. Diesel Locomotives 10:1–3 (in Chinese)
2. Liu Y (2012) New energy strategy thinking about rail power traction. Electr Locomotives
   Mass Transit Veh 35(5):1–4 (in Chinese)
3. Ye D, Peng C, Liu S (2012) The development of hybrid traction shunting locomotive. Electr
   Drive Locomotives 5:17–20 (in Chinese)
4. Tiant Z (2011) Japan HD300-901 type hybrid locomotive prototype. Foreign Diesel
   Locomotive 5:10–14 (in Chinese)

5. Ma X, Gao D (2012) Application feasibility study on power lithium-ion battery for double energy locomotive. Electr Locomotives Mass Transit Veh 35(6):53–56 (in Chinese)
6. Heesung P (2013) A design of air flow configuration for cooling lithium ion battery in hybrid electric vehicles. J Power Sources 239:30–36
7. Sungjin P, Dohoy J (2013) Battery cell arrangement and heat transfer fluid effects on the parasitic power consumption and the cell temperature distribution in a hybrid electric vehicle. J Power Sources 227:191–198
8. Li X, He F, Ma L (2013) Thermal management of cylindrical batteries investigated using wind tunnel testing and computational fluid dynamics simulation. J Power Sources 238:395–402
9. Xun J, Liu R, Jiao K (2013) Numerical and analytical modeling of lithium ion battery thermal behaviors with different cooling designs. J Power Sources 233:47–61